

Supplementary Information

Orchestrated photocatalytic hydrogen generation using surface-adsorbing iridium photosensitizers

Yan-Jie Wang,^a Gang Chang,^b Qingyun Chen,^c Guan-Jun Yang,^d Sheng-Qiang Fan*^b and Baizeng Fang*^a

^a Department of Chemical & Biological Engineering, University of British Columbia, 2360 East Mall, Vancouver, B.C., Canada V6T 1Z3. E-mail: bfang@chbe.ubc.ca; Tel: +1 604-8273232

^b Department of Chemistry, School of Science, Xi'an Jiaotong University, Xi'an, Shaanxi 710049, P. R. China. E-mail: fsq@mail.xjtu.edu.cn; Tel: +86 29 82663914

^c State Key Laboratory of Multiphase Flow in Power Engineering, Xi'an Jiaotong University, Xi'an, Shaanxi 710049, P. R. China.

^d State Key Laboratory for Mechanical Behavior of Materials, Xi'an Jiaotong University, Xi'an, Shaanxi 710049, P. R. China.

Illustrated Photocatalytic Hydrogen Generation

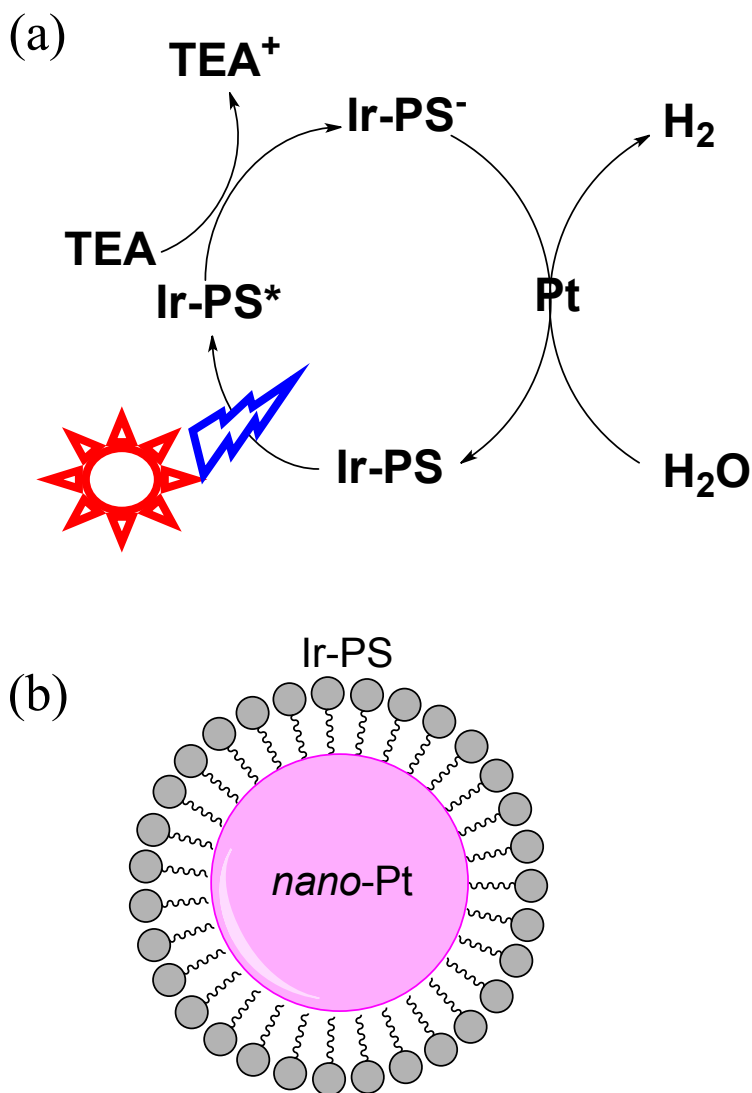


Figure S1 (a) Schematic water reduction process and (b) orchestrated structure of Ir-PS molecules on Pt nano-particles. TEA stands for triethylamine, Ir-PS for the photosensitizer, Ir-PS* for the excited state, and Ir-PS⁻ for the reduced state.

Experimental Details

Compound **3** was purchased from Alfa. Compounds **2** and **5** were synthesized following literature procedures.¹ All reagents were used as received. Anhydrous solvents for analysis were distilled over Na/benzophenone.

Compound **1**. A mixture of 7-bromo-9,9-dipropyl-9H-fluorene-2-carbaldehyde² (357 mg, 1.0 mmol), bis(pinacolato)diboron (305 mg, 1.2 mmol), potassium acetate (98 mg, 3.0 mmol), (1,1'-bis(diphenylphosphino)ferrocene)dichloropalladium(II) (22 mg, ~0.03 mmol), and 1,4-dioxane (10 mL)

was deoxygenated and then heated at 100 °C under argon for 6 h. During the reaction, the color of the mixture changed from yellow to dark gradually. After the mixture was cooled to room temperature, 1,4-dioxane was completely removed under vacuum. Then dichloromethane (50 mL) and water (50 mL) were added to the solid mixture, and the two layers were separated. The aqueous layer was extracted with dichloromethane (3×50 mL), and then the organic layer and extracts were combined, dried over anhydrous magnesium sulfate, and filtered. The solvent was completely removed and the residue was purified by column chromatography over silica gel using ethyl acetate/light petroleum (1:3) as eluent to give **1** as a white solid (308 mg, 76%); mp 117 °C. ¹H NMR (400 MHz, CDCl₃): δ 0.55-0.65 (m, 10H), 1.39 (s, 12H), 2.01-2.05 (m, 4H), 7.76-7.79 (m, 2H), 7.83-7.85 (m, 3H), 7.89 (t, 1H, J=0.96), and 10.06 (s, 1H). *m/z* [ESI]: 427.2 ([M+Na]⁺). Anal. Cal. For C₂₆H₃₃BO₃: C, 77.2; H, 8.2. Found: C, 77.3; H, 8.3

General protocol for the synthesis of formyl bipyridyl ligand. The respective bromobipyridine (**2** and **5**, typically 0.33 mmol), boronate compound (**1** and **3**, 1.3 equivalent to –Br function), sodium carbonate (2 M aqua, 3 mL), Pd(PPh₃)₄ (3% mol of –Br function) and tetrahydrofuran (25 mL) were refluxed under argon for 48 h. When cooled, the organic layer was separated and the aqueous layer was extracted with ethyl acetate (3×20 mL). The organic portions were combined, dried and purified by column chromatography over silica gel using dichloromethane/ethyl acetate (1:0 to 1:1) as eluent.

Compound **3** (yield 65%): mp 276-277 °C. ¹H NMR (400 MHz, CDCl₃) δ 0.65-0.72 (m, 20H), 2.08-2.12 (m, 8H), 7.67 (dd, 2H, J=5.08 & 1.84), 7.80 (d, 2H, J=1.12), 7.83 (dd, 2H, J=7.88 & 1.56), 7.90-7.93 (m, 8H), 8.81-8.84 (m, 4H), 10.09 (s, 2H). *m/z* [ESI]: 709.5 ([M+H]⁺). Anal. Cal. For C₅₀H₄₈N₂O₂: C, 84.71; H, 6.82; N, 3.95. Found: C, 84.92; H, 6.93; N, 4.05.

Compound **6** (yield 92%): mp 180-181 °C. ¹H NMR (400 MHz, CDCl₃) δ 7.33 (m, 1H), 7.79-7.86 (m, 3H), 7.98-8.01 (m, 2H), 8.05 (dd, 1H, J=8.24 & 2.36), 8.44 (d, 1H, J=7.96), 8.51 (d, 1H, J=8.28), 8.70 (m, 1H), 8.94 (d, 1H, J=1.80), 10.07 (s, 1H). *m/z* [ESI]: 283.1 ([M+Na]⁺). Anal. Cal. For C₁₇H₁₂N₂O: C, 78.44; H, 4.65; N, 10.76. Found: C, 78.67; H, 4.55; N, 10.91.

General protocol for the synthesis of Ir-PSs. A mixture of iridium dimer [Ir(ppy)₂Cl]₂³ (0.05 mmol) and the respective bipyridyl ligand (0.10mmol) in dichloromethane/methanol(10 mL/6 mL) was stirred at 55 °C under Ar for 16 h. After cooled, the solvent was removed and the residue was dissolved in 10 mL of methanol. Then KPF₆ (1 mmol) in 10 mL H₂O was added to get red precipitates, which was then filtered and purified through recrystallization by vapor diffusion of diethyl ether to the dichloromethane solution of the crude.

4-FICHO-Ir (yield 89%):¹H NMR (400 MHz, CDCl₃) δ 0.52-0.65 (m, 20H), 2.10-2.15 (m, 8H), 6.29 (dd, 2H, J=7.60 & 0.88), 6.97 (dt, 2H, J=7.40 & 1.08), 7.07 (dt, 2H, J=8.52 & 1.08), 7.21 (dt, 2H, J=7.28 & 1.16), 7.83 (d, 2H, J=5.80), 7.92 (d, 2H, J=5.88), 7.95-7.95 (m, 6H), 8.04 (s, 2H), 8.19-8.26

(m, 10H), 8.32 (d, 2H, J=8.36), 9.41 (s, 2H), 10.09 (s, 2H). *m/z* [ESI]: 1209.5 ([M-PF₆]⁺). Anal. Cal. For C₇₂H₆₄F₆IrN₄O₂P: C, 63.84; H, 4.76; N, 4.14. Found: C, 63.64; H, 4.55; N, 4.02.

3-PhCHO-Ir (yield 76%): ¹H NMR (400 MHz, CDCl₃) δ 6.33-6.36 (m, 2H), 6.92-6.97 (m, 2H), 7.04-7.09 (m, 4H), 7.42-7.49 (m, 3H), 7.56 (d, 1H, J=5.52), 7.60 (d, 1H, J=5.36), 7.70-7.73 (m, 2H), 7.78 (dt, 2H, J=7.56 & 2.68), 7.89-7.97 (m, 5H), 8.14-8.18 (m, 2H), 8.47 (m, 1H), 8.84-8.94 (m, 2H), 10.02 (s, 1H). *m/z* [ESI]: 761.2([M-PF₆]⁺). Anal. Cal. For C₃₉H₂₈F₆IrN₄OP: C, 51.71; H, 3.12; N, 6.19. Found: C, 52.01; H, 3.24; N, 6.03.

Characterization. UV-vis absorption spectra were recorded on a Cary 500 UV-Vis spectrophotometer. Steady-state photoluminescence (PL) was recorded on a SENS-9000 spectrophotometer. Time-resolved PL was carried out using QM4 with time correlated single photon counting (TCSPC) capability. Cyclic voltammetry (CV) measurements were performed using BASi Epsilon-EC work station with anhydrous THF as solvent, glass carbon as working electrode, platinum wire as counter electrode, Ag/AgNO₃ (0.1 M) as reference electrode, ⁿBu₄NBF₆ (0.1 M) electrolyte and ferrocene standard, at a scan rate of 100 mV/s. The incident photon to hydrogen conversion efficiency (IPCE) was determined by dividing the rate of evolved hydrogen gas with the flux of incident photons at a specific wavelength. A high pressure mercury lamp (LLE-9, 50 W) was employed as light source and the light output was adjusted to 1.0 W for 365, 405, 436, 492 and 546 nm, respectively, with the assistance of light filters. The power output was determined by a radiometer (FZ-A).

Procedures for hydrogen evolution experiment. The H₂-generation efficiencies of the Ir(III) complexes PS were evaluated in a mixture of 0.50 μmol of PS, 0.30 μmol of K₂PtCl₄, 2 mL of TEA, 2 mL of H₂O, and 6 mL of THF, using a 150 W Xeon lamp as the light source. Colloidal Pt catalyst was *in situ* formed from K₂PtCl₄ in the solution.⁴ The amount of evolved gas was measured with an automatic gas burette, and gas compositions were analyzed by GC (Shimadzu).

Table S1 Photophysical and electrochemical characteristics, and the TONs of photocatalytic hydrogen generation for 4-FI-Ir.⁵

Ir(III) complex	λ _{em} ^a (nm)	E _g (opt) ^b (eV)	φ _{PL} ^c	τ ^d (μs)	E(PS [•] /PS ^e) (V)	E(PS/PS [•]) ^f (V)	E(PS*/PS) ^g (V)	V(H ₂) ^h (mL)	TON ⁱ
4-FI-Ir	602	2.33	0.45	0.53	+1.54	-1.08	+1.25	-	1,735

^a Emission peak in CH₂Cl₂; ^b optical bandgap from the crossover of UV-vis and PL spectra; ^c excited at 350 nm in degassed THF using quinine sulphate as reference; ^d excited-state lifetime; ^e oxidation potential; ^f reduction potential; ^g excited-state oxidation potential, calculated by E(PS/PS[•])+E_g(opt); ^h The reaction mixtures contained 0.5 μmol of Ir-PS, 0.30 μmol of K₂PtCl₄, 2 mL of TEA, 2 mL of H₂O, and 6 mL of THF; ⁱ n(H)/n(PS).

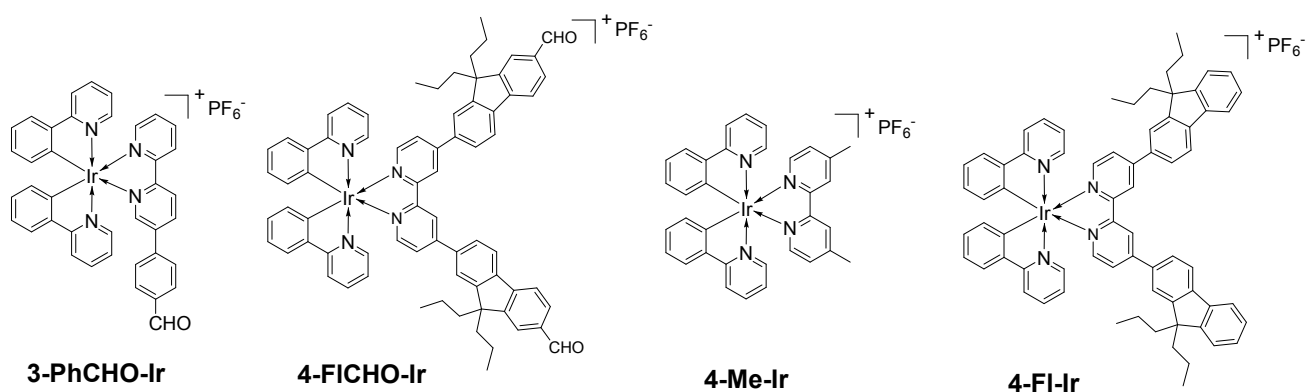


Figure S2 Molecular structures of two new formyl Ir-PSs, **3-PhCHO-Ir** and **4-FICHO-Ir**, together with two model Ir-PSs, **4-Me-Ir**⁴ and **4-FI-Ir**⁵.

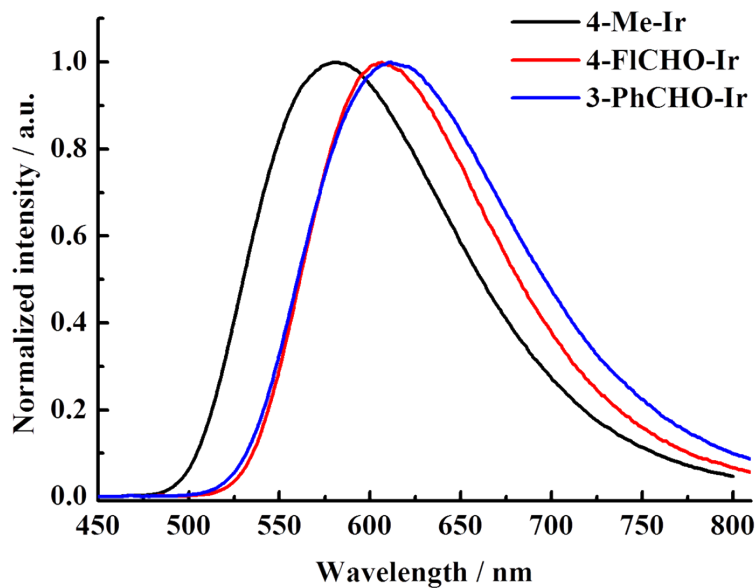


Figure S3 Photoluminescence spectra of Ir-PSs in argon saturated CH_2Cl_2 at room temperature, excitation = 410 nm.

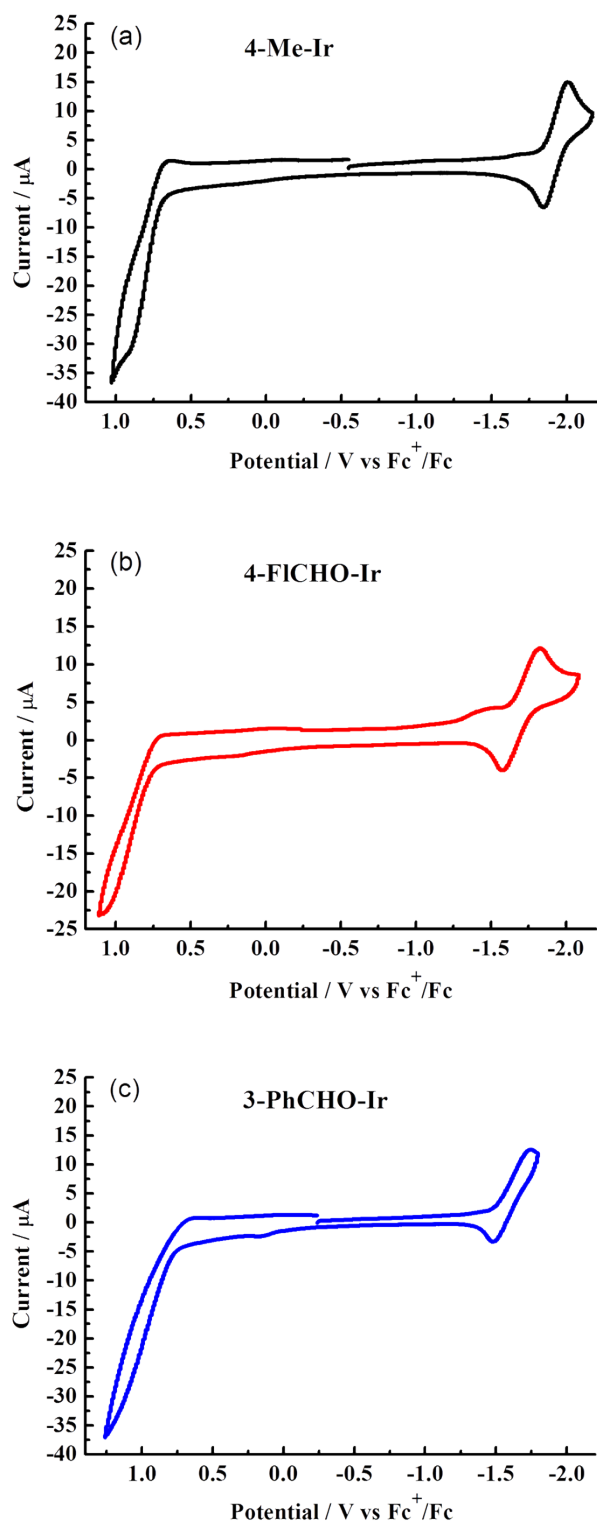


Figure S4 CV plots of the Ir-PSs measured in anhydrous THF with glass carbon as working electrode, platinum wire as counter electrode, Ag/AgNO_3 (0.1 M) as reference electrode, $n\text{Bu}_4\text{NBF}_6$ (0.1 M) electrolyte and ferrocene standard, at a scan rate of 100 mV/s.

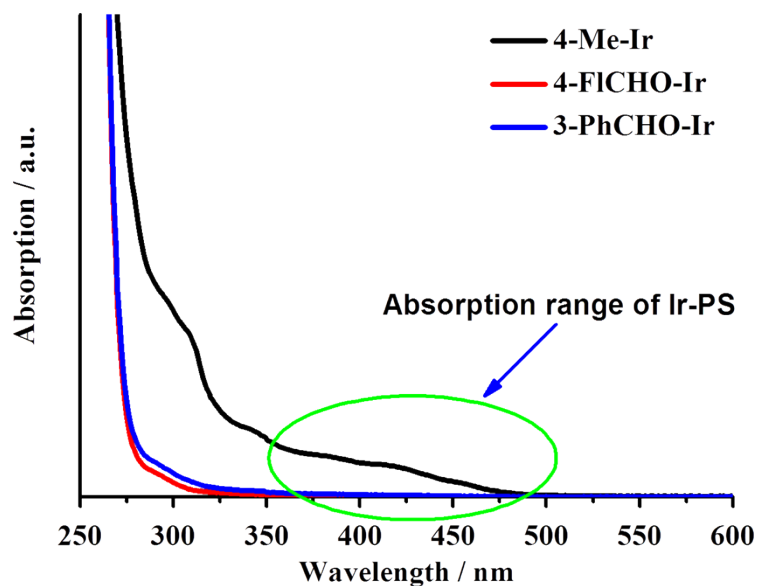


Figure S5 UV-vis absorption spectra of the Ir-PSs after photoreactions. The photoreactions were carried out with 0.1 μmol of Ir-PS and 0.50 μmol of K_2PtCl_4 in TEA/ H_2O /THF (2.0 mL/2.0 mL/6.0 mL). The residues after 1 h hydrogen-generation reactions were filtered through a syringe filter (0.2 μm pore size), and then the filtrates were analysed in UV-visible spectrometer.

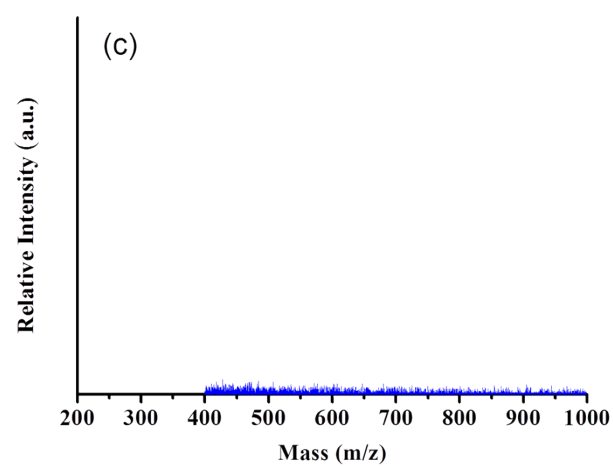
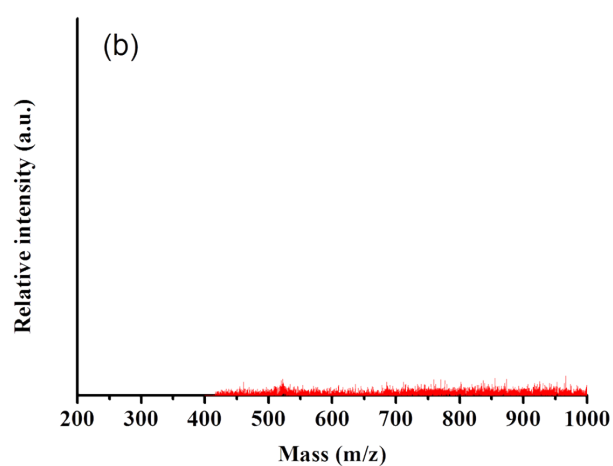
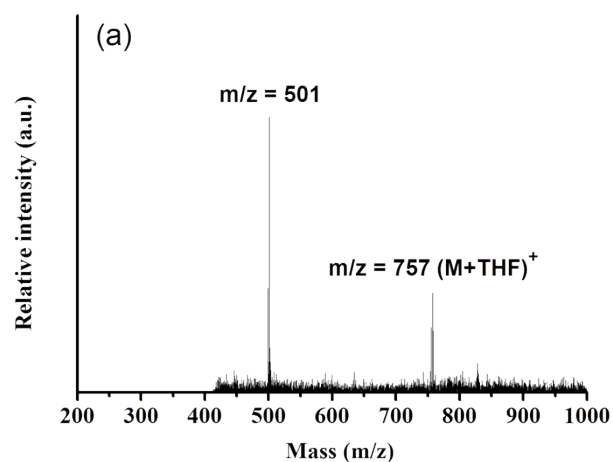


Figure S6 Mass spectra of **4-Me-Ir** (a), **4-FICHO-Ir** (b), and **3-PhCHO-Ir** (c) after the photoreaction. The photoreaction was carried out with 0.1 μmol of Ir-PS and 0.50 μmol of K_2PtCl_4 in TEA/ H_2O /THF (2.0 mL/2.0 mL/6.0 mL). The residue after 1 h hydrogen-generation reactions were filtered through a syringe filter (0.2 μm pore size), and then the filtrate was analysed in ESI-MS.

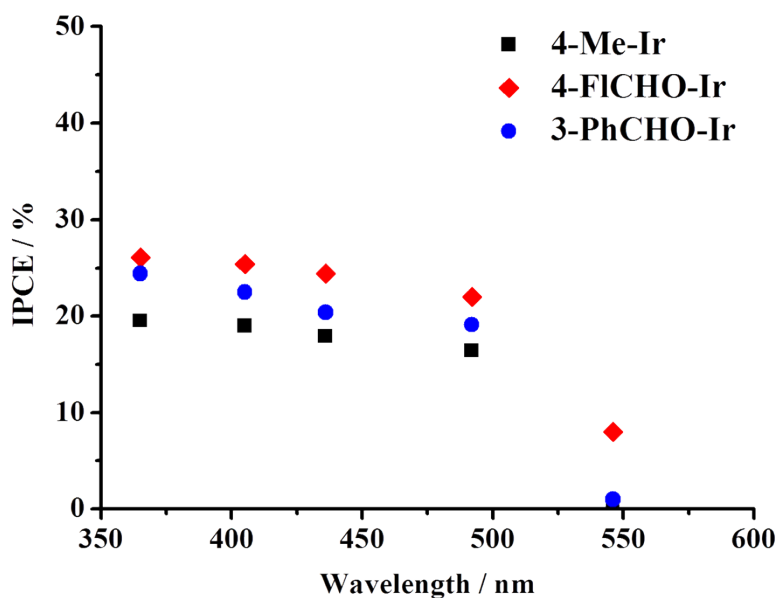


Figure S7 IPCE shown as a function of wavelength for the various Ir-PSs. The photoreactions were carried out using 20 μmol of PS, 0.30 μmol of K_2PtCl_4 , 2.0 mL of TEA, 2.0 mL of H_2O and 6.0 mL of THF.

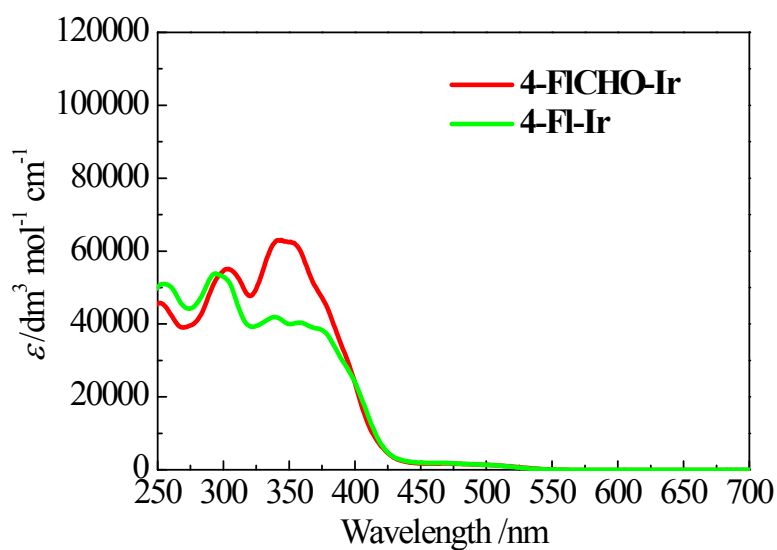


Figure S8 Comparison of UV-Vis absorption spectra of the two Ir-PSs, 4-FI-CHO-Ir and 4-FI-Ir⁵.

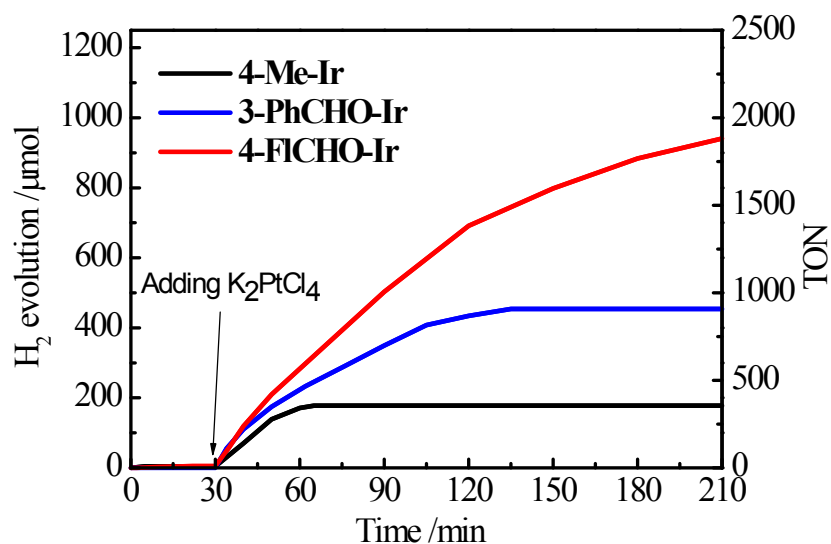


Figure S9 Kinetic traces of H₂-generation photoreactions for different Ir-PSs under controlled conditions: first, the reaction mixtures contained 0.5 μmol of Ir-PS, 2 mL of TEA, 1 mL of H₂O, and 6 mL of THF were illuminated by Xe light source for 30 min; second, 0.30 μmol of K₂PtCl₄ in 1 mL of H₂O was added and the resultant mixtures were kept under light illumination. The results reveal that without Pt catalyst hydrogen generation amounts are close to zero for all these three Ir-PSs. When K₂PtCl₄ was added after 30 min of illumination, hydrogen was generated. However, the TON is much lower than non-controlled reactions, suggesting that without Pt catalyst Ir-PSs degrade in the system faster. This can be ascribed to the slow quenching of Ir-PS⁻ in the absence of Pt catalyst. This result reflects the importance of the enhanced Ir-PS/Pt interaction for fast quenching of Ir-PS⁻.

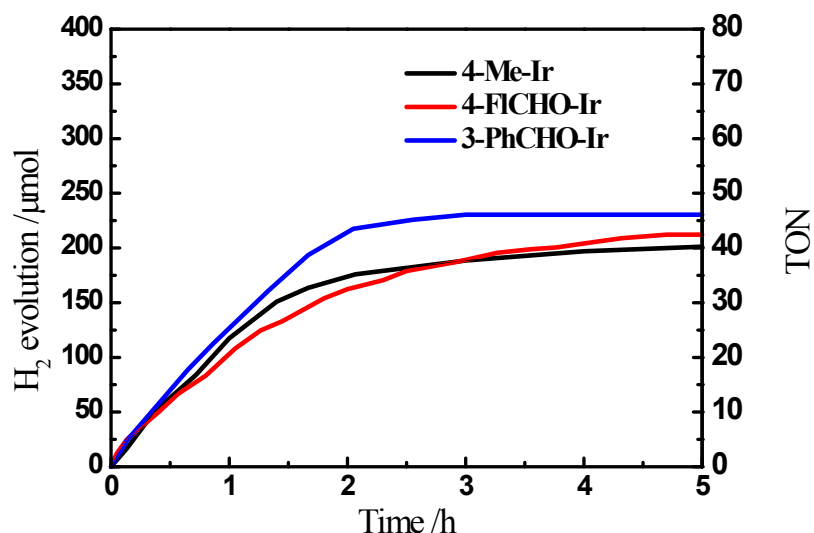


Figure S10 Kinetic traces of H₂-generation photoreactions for different Ir-PSs with molecular Co(bipyridyl)₃(PF₆)₂ catalyst. The reaction mixtures contained 10 μmol of Ir-PS, 10 μmol of Co(bipyridyl)₃(PF₆)₂, 1 mL of triethanolamine, 3 mL of H₂O, and 6 mL of acetonitrile. In these molecular catalyst-based photoreactions, the advantage of the formyl Ir-PSs over the non-formyl Ir-PS is not seen clearly.

References

- 1 W.-S. Han, J.-K. Han, H.-Y. Kim, M.-J. Choi, Y.-S. Kang, C. Pac, S.-O. Kang, *Inorg. Chem.*, 2011, **50**, 3271–3280.
- 2 C.-L. Chiang, M.-F. Wu, D.-C. Dai, Y.-S. Wen, J.-K. Wang and C.-T. Chen, *Adv. Func. Mater.*, 2005, **15**, 231–238.
- 3 F. Gärtner, D. Cozzula, S. Losse, A. Boddien, G. Anikumar, H. Junge, T. Schulz, N. Marquet, A. Spannenberg, S. Gladiali and M. Beller, *Chem. Eur. J.*, 2011, **17**, 6998–7006.
- 4 P. N. Curtin, L. L. Tinker, C. M. Burgess, E. D. Cline and S. Bernhard, *Inorg. Chem.*, 2009, **48**, 10498–10506.
- 5 S. Fan, Cyclometallated Iridium(III) Complexes for Photocatalytic Water Splitting Applications, PhD Thesis, 2013, the University of Queensland.